Available online at www.sciencedirect.com
SCIENCE DIRECT®
C. R. Physique 4 (2003) 1047–1054
COMPTES RENDUS PHYSIQUE

Carbon nanotubes: state of the art and applications/Les nanotubes de carbone : état de l'art et applications

Thermal properties of carbon nanotubes

Jean-Claude Lasjaunias

Centre de recherches sur les très basses températures, CNRS, laboratoire associé à l'Université Joseph Fourier, BP 166, 38042 Grenoble cedex 9, France

Presented by Guy Laval

Abstract

Thermal properties, such as thermal transport, heat capacity and its relation to elastic constants, and He adsorption, are presented by comparing theoretical predictions, in general for individual C-nanotubes (NT), to some typical experimental results commonly obtained not on individual NTs, but on larger collective arrangements, such as multiwalled NT or singlewalled NT ropes. ***To cite this article: J.-C. Lasjaunias, C. R. Physique 4 (2003).***

Résumé

Les propriétés thermiques des nanotubes de carbone. Nous présentons des propriétés thermiques telles que le transport thermique, la chaleur spécifique en relation avec les constantes élastiques, ou l'absorption d'He, en comparant les prédictions théoriques obtenues en général pour les nanotubes (NT) individuels, avec quelques résultats expérimentaux typiques obtenus en général non sur des NT individuels, mais sous forme d'arrangements de NT multi-parois, ou de faisceaux de NT mono-parois. ***Pour citer cet article : J.-C. Lasjaunias, C. R. Physique 4 (2003).***

1. Introduction

Twelve years after their discovery, C-nanotubes (NT) seem very promising materials, in particular for mechanical and electronic applications, and possibly for gas storage. However, although individual nanotubes show, or are expected to show, many exceptional physical properties due to their genuine 1D carbon-based structure, the need for large amount of materials for industrial applications, for instance as composite materials for mechanical applications, is often a severe limitation, since a macroscopic arrangement of NTs, at first in NT bundles, or in the form of arrays of multiwalled NT or fibres, generally leads to a degradation of their initial exceptional properties. In addition, these properties seem to be very sensitive to the method of preparation. In the following, I intend to show by a few examples, the gap between the theoretical predictions or the few measurements realized on individual NTs using a high technological support (mesoscopic physics) and the more usual experiments performed on a larger amount of material.

2. Thermal transport properties

We consider here that the thermal conductivity $\kappa(T)$ in the presently investigated temperature range from $\sim$10 K to 300–400 K. $\kappa(T)$ reduces, at least above 10 K, to the phonon contribution since the electronic contribution is estimated to be two orders of magnitude smaller. Contrary to the case of the heat capacity, discussed later, transport measurements, either electrical or thermal, are very sensitive to the morphology or geometry of the samples, and also to the thermal resistance between different

E-mail address: lasjau@labs.polycnrs-gre.fr (J.-C. Lasjaunias).

1631-0705/$ – see front matter
doi:10.1016/S1631-0705(03)00112-9

portions of the sample itself, and between the sample and the external thermal sink. This can partly explain the wide spread of data obtained in the last 3 years. The first pioneering work [1] was made on as-prepared, millimetric size, 'mat' samples of tangled NT bundles. $\kappa(T)$ (Fig. 1) increases regularly up to 350 K, with a linear-in-T behaviour below 25 K. An estimated value at room temperature (RT) was 35 W/m · K. Despite the fact that measurements were performed on a macroscopic system, the authors proposed an appealing interpretation in terms of one-dimensional phonon bands, and an estimation of the phonon mean free path in agreement with the length of bundles (∼1 µm). Later, molecular dynamics simulations [2] predicted for isolated NTs a totally different behaviour (Fig. 2), κ being dominated by phonon Umklapp scattering processes above 100 K, at the origin of a maximum of 4×10^4 W/m · K at 100 K, and decreasing to 6600 W/m · K at RT, i.e., about 2–3 times larger than pure diamond or in-plane conductivity of graphite, which are the largest in solid state physics. Improvement of the sample geometry/morphology was achieved in two later reports. In [3] with millimeter long, aligned MWNTs: the tubules grow out perpendicularly from the substrate, forming a highly aligned array. $\kappa(T)$ shows a quadratic regime up to 100 K, a qualitative behaviour confirmed by further research, and linear-in-T above 100 K, to reach 25 W/m · K at RT. The data, including the specific heat calculated from the thermal diffusivity, were compared to that of graphite. In [4] the authors measured SWNT ropes, preferentially aligned (to a fraction of 70–80%) by filter deposition from suspension in strong magnetic fields. As expected (see Fig. 3) there is a large anisotropy of κ, essentially similar to that of electrical resistivity, depending on the orientation of the heat flow Q perpendicular or parallel to the field alignment. An interesting point for possible practical applications is that the alignment effect under a 7 T field is almost the same as with a 26 T field. The variation of κ is quite similar to that of previous work, with an absolute value at RT of about 40 W/m · K, for Q ∥ H. Note that the previous value (25 W/m · K [3]) is just intermediate between the two present extreme values, for Q ∥ or ⊥ H.

Finally, recent mesoscopic measurements using electron beam lithography processes, were realized on an *individual* MWNT, typically 14 nm in diameter, which forms a thermal path between two suspended islands, by means of silicon nitride legs [5, Fig. 4]. There were several assumptions and simplifications concerning the estimation of the thermal resistance of the junctions, the possible role of radial anisotropy of the multi-walls, and the problem of exact determination of the geometrical factor, in order to extract the absolute value. However, the correction for radiation losses is not explicitly mentioned in the papers. The authors could conclude a RT value of 3000 W/m · K, comparable to the initial theoretical expectations. Following a low-T ($T > 10$ K) close to quadratic T^2 regime, a maximum occurs at 300 K, which could indicate the U-processes also theoretically expected. They also estimate a constant phonon mean free path below the maximum, of ∼0.5 µm, comparable to the length of the MWNT (2.5 µm), and for the T range 50–150 K, a quadratic regime, somewhat similar to the graphite behaviour. In conclusion, the authors ascribe the differences between mesoscopic and 'bulk' measurements to "numerous highly resistive thermal junctions between different tubes" which can dominate the thermal transport in mat samples, and also to the estimation of sample dimensions.

At this step it will be interesting to compare more precisely these MWNT data to those of bulk crystalline graphite, in particular to in-plane conductivity of high crystalline quality: heat-treated pyrolytic graphite (see references quoted in paper [2]). There are certain similarities for the power-law dependence of $\kappa(T)$, which evolves from $T^{2.5-2.6}$ to T^2 in the T-range from 10 K to 50 K in both cases (which hints for a 2D behaviour for MWNTs too [5]), as well as for the maximum values: κ reaches $4–5 \times 10^3$ W/m · K for $T_m \sim 100–150$ K for in-plane κ in graphite, compared to 3×10^3 in NTs, but with T_m shifted to around 300 K. In contrast, the amplitude of κ below ∼100 K is reduced by more than one order of magnitude in NTs, in comparison

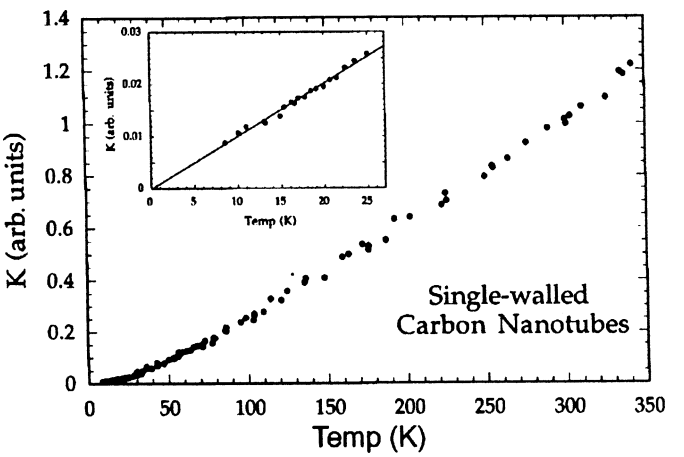

Fig. 1. Temperature dependent thermal conductivity of SWNT (from [1], with the authors' permission; originally published by the American Physical Society).

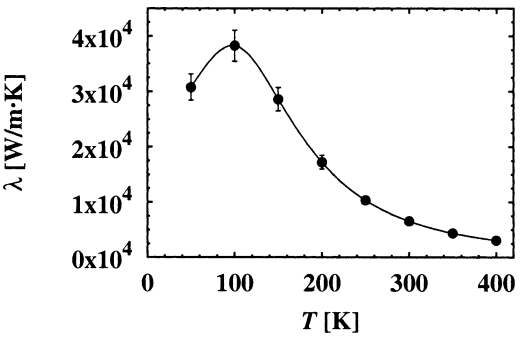

Fig. 2. Temperature dependence of the thermal conductivity for a (10, 10) carbon nanotube for T below 400 K (from [2], with the permission of the first author; originally published by the American Physical Society).

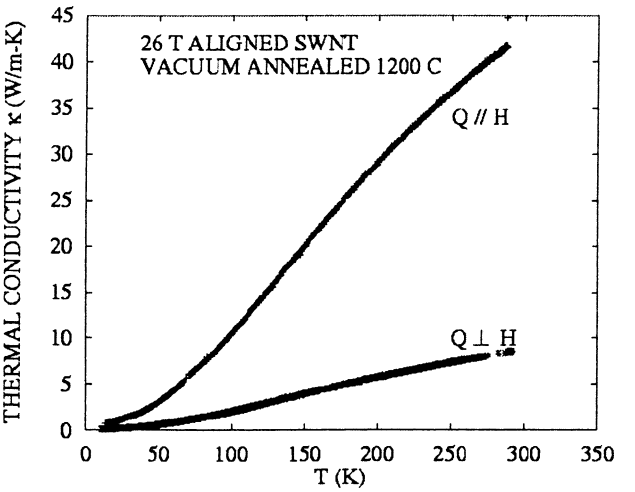

Fig. 3. Thermal conductivity of annealed 26 Tesla-aligned SWNT films measured with heat flow perpendicular and parallel to the alignment axis (from [4], with the permission of the first author; originally published by the American Institute of Physics).

to graphite. Within the usual 3D or 2D interpretation, low-T κ is determined by boundary scattering, either by defects or the crystallite size d. In the case of basal-plane conductivity of graphite, the amplitude of the quasi-quadratic regime can also be determined by this crystallite size d. For the best quality samples, d was estimated to a few tens of μm, either theoretically or experimentally (see Ref. [19] quoted in paper [2]). One can outline that there is almost the same difference, by one order of magnitude, between the overall length of the MWNT sample – 2.5 μm – and the d value for graphitic planes. Therefore, it will be of great interest to test low-T (<100 K) κ, using the same technique, on much longer samples, and verify if it can reach the graphite 2D value.

We can conclude, if the high κ value measured in the mesoscopic measurements is confirmed, that as in the case of elastic or mechanical properties reported in the following section, the use of 'bulk' arrangements of NTs, even in an oriented configuration of aligned bundles, is a severe limitation of the exceptional properties of individual NTs, for a possible application with the need for large masses. Indeed, very sophisticated technology is necessary to benefit from the exceptional properties of NTs.

We note that the experiments below 10 K are still lacking, in a T-range where the phonon quantization due to the 1D structure could yield a specific 'quantum regime' for the phonon transport at low T, which is of the order of $(h/2\pi)v/R$, with v the sound velocity, and R the radius of nanotube. Recent preliminary experiments [6] using sophisticated mesoscopic techniques on 1D nanostructures (not nanotubes), which are severely limited by any parasitic power input of the order of 10^{-16} W or less, appear to bring evidence of such a quantum regime below 0.8 K. Such properties could only be tested in *individual* NTs since, as for the heat capacity, in the case of ropes or MWNTs the purely 1D phononic properties are masked by the increasing transversal phonon coupling on lowering T. However, due to the really nanometric scale of individual NTs (∼1.4 nm), one should expect an extension of phonon quantization to about 10 K, whereas for MWNT it is limited to 1 K [6].

3. Heat capacity and elastic constants

Indeed, the paper of Hone et al. [7] which reports on the specific heat of SWNT ropes between 2 and 300 K is focused on the 1D behaviour, and especially at low T (below ∼10 K), where the phonon quantization for strictly 1D structures should lead to a linear-in-T variation. Their data (Fig. 5) are interpreted over a wide T interval (above 5 K) with a strictly 1D model which implies: (a) a constant density of states for acoustic phonons at very low energy; (b) successive peaked van Hove singularities in the DOS, the result of quantized phonon subbands, similar to the electronic band structure. However, contrary to the authors' claim, I think that these data do not bring the proof of phonon quantum effects. In fact, there is some inconsistency between the log–log plot in their Fig. 3 (here Fig. 5), where no linear variation is observable, especially below 5 K, whereas a continuous power $T^{1.6}$ law can well fit the data between 2 and 20 K, and the linear plot in their Fig. 4 (here Fig. 6), where C_p is shown to vary linearly from 2 to 8 K. In this second plot, the linear regime for acoustic phonons is restricted to the range 2–6 K, and in addition C_p cannot extrapolate linearly to zero T in an usual way: there is a crossover at $T = 2$ K to a different regime. The authors admit, from the log–log plot, that the data deviate below 5 K from the isolated tube prediction (the linear regime

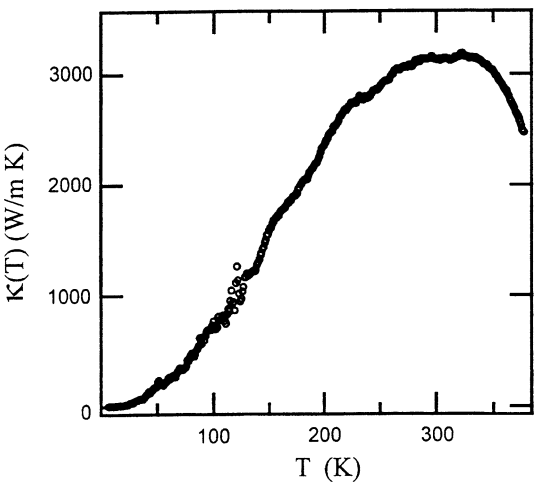

Fig. 4. The T-dependent thermal conductivity of an individual MWNT of a diameter 14 nm (from [5], with permission of Elsevier).

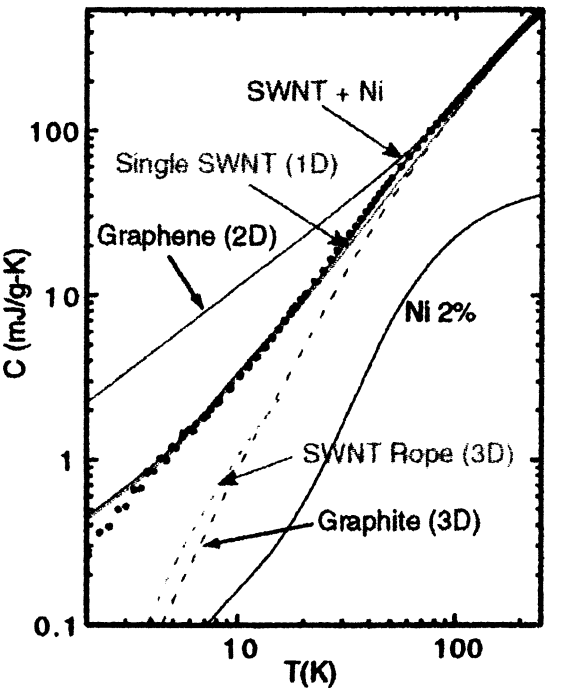

Fig. 5. Log–log plot of specific heat data of a sample consisting mainly of SWNT ropes (solid dots) compared with calculations for 2D graphene, 3D graphite, isolated tubes, and strongly coupled ropes. The data agree with the isolated tube model down to 5 K. (Reprinted with permission from Hone et al., Science 289 (2000) 1730. Copyright 2000 American Association for the Advancement of Science.)

down to zero), and that it is the effect of elastic transversal coupling between adjacent tubes of the bundle which take over on the longitudinal 1D modes at very low temperatures. It is difficult to reconcile the scheme of a phonon DOS with a first sharp subband peak at 4.2 meV (which begins to contribute to C_p at 8 K), and a constant DOS down to 1.2 meV (the crossover towards the 3D bundle lattice regime below 4 K) with a so monotonous, power law variation shown in Fig. 5.

The dimensionality crossover from a high temperature quasi-1D behaviour to a low-T 3D behaviour, which depends on the transversal elastic coupling between the tubes in the bundle, is a well known problem in quasi-1D materials with chain-like structures, such as polymers or 1D conductors in the Peierls state: there always occurs a 3D cubic regime in the heat capacity at sufficiently low T, depending on the anisotropy of force constants along the chains and between them [8]. In the case of the rather weak Van der Waals binding between NTs in a bundle, one can expect a rather low T_{CO} crossover value. Indeed, our own measurements on similar samples extended in a lower T range down to 100 mK have clearly revealed the 3D phonon regime expected below a few K (see Figs. 7 and 8). In the case of the same samples as in [7], the T^3 regime extends up to 4.5 K, then turning to a less rapid variation, perhaps in T^2. We could not draw any conclusion about phonon quantization from the C_p data below 7 K, since it is rapidly determined by the 3D morphology of the bundles. The existence of possible van Hove singularities seems difficult to establish from the calorimetric experiments, due to the smearing out effect of sharp accidents in the phonon DOS by the Bose statistics; except for the lowest subband energy E_{SO} which will induce a rapid decrease of C_p for $kT \ll E_{SO}$, which is not seen in the reference data [7]. On the other hand, the absence of singularities in the DOS is confirmed by inelastic neutron scattering experiments, which show a very monotonous variation of the generalized DOS, $G(E)$, generally linear in E between 0.3 meV and at least 1.3–1.5 meV – corresponding for C_p to a temperature between 0.8 K and 4 K – with a change of slope, but with no peaks, around 1.5–2 meV, for different samples [9,10].

Consequently, as for the thermal transport, the specific heat will unambiguously reveal the specific 1D properties like phonon quantization, if measurements are done on individual NT, which is another technical challenge, but probably resolved in the near future.

Now we can consider our specific heat investigation on two kinds of SWNT bundles, which essentially differ in the bundle sizes that may have implications for the low-energy vibrational states, and also for related properties like gas adsorption, such

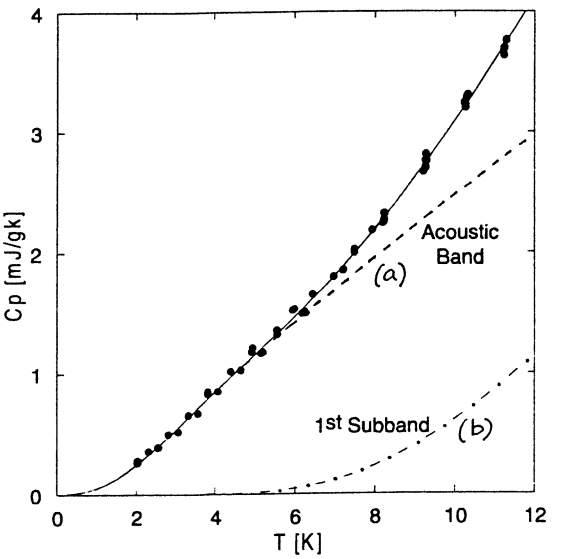

Fig. 6. The same data as in Fig. 5, in an expanded linear scale, and a fit to an anisotropic two-band Debye model that accounts for weak coupling between SWNTs in a rope. (a) represents the contribution from acoustic modes in the 1D model; (b) represents the contribution of the first subband, approximated as a dispersionless optic branch at energy E_{sub}. These two are combined in the black curve which fits the data over the entire range. (Reprinted with permission from Hone et al., Science 289 (2000) 1730. Copyright 2000 American Association for the Advancement of Science, and Z. Benes, Thesis, 2001.)

as He^4 (see below). These samples were prepared either by laser vaporization technique (LV in short), known as the 'Rice' technique [11] in the form of mat-buckypaper foils, or by electric arc discharge (AD in short) from the Montpellier group [12], in the form of a pressurized (at 10 kbar) powder pellet. The measured mass was 45 and 90 mg respectively. Both consist of NTs of 1.4 ± 0.2 nm in diameter, arranged in bundles of less than 10 nm (i.e., $\leqslant 30$ tubes) for AD, but extending from 5–10 nm up to 20 nm or more (i.e., 100 tubes or more) for LV sample.

Raw data of the LV sample [13] are reported in Fig. 7 for different amounts of adsorbed He^4 gas, in concentrations estimated to ~3 at. % of C atoms in run B (maximum adsorption), ~0.1 at. % in run A, and totally outgassed in run C, which therefore represents the pristine NT state. We have a numerical agreement for data of this run C with previous results of Hone et al. [7] at $T = 2$ K, and with those of Mizel et al. [14] for T below 3 K, both on SWNT ropes. We note the large, measurable contribution of He in this T range. This property was previously observed in one run extended to 25 K [7]. Another large, extrinsic, contribution is the hyperfine nuclear T^{-2} term, which becomes predominant below 0.2 K. It originates from the residual ferromagnetic catalyst particles, here 0.7 to 1 at. % Co. So, the low-T heat capacity is also a sensitive sensor to ferromagnetic catalysts. Once this well defined nuclear term C_{N} has been subtracted, one obtains the vibrational contribution, since the electronic one is about two orders of magnitude smaller. This contribution, reported in Fig. 8 as $C_{\mathrm{p}} - C_{\mathrm{N}}$, is analysed as the sum of a sub-linear $T^{0.62}$ term, ascribed to localized excitations due to structural defects of the NT, or to their porosity, and a well defined T^3 term over more than 3 decades in C_{p}, from 0.3 to 4.5 K: this corresponds to the 3D propagative phonon contribution. The crossover to a weaker power law variation above $T_{\mathrm{CO}} = 4.5$ K suggests the phonon dimensionality crossover discussed above. Within the dominant phonon approximation, this corresponds to an energy of 1.7 meV. This is a direct measure of the inter-tube coupling strength, equivalent to a transverse Debye energy, above which transverse phonons are frozen out. It is above this energy that one expects 1D (or 2D?) behaviour for a bundle geometry. In the previous work [7], the low-T deviation from the 1D model below 2–5 K (but without the evidence of a cubic regime) was ascribed to a crossover energy estimated to 1.2 meV.

From the amplitude of the βT^3 contribution one can directly extract a mean Debye sound velocity v_{D}, and an estimation of the effective transverse velocity, v_{T}, if one supposes – a reasonable assumption – that it is much smaller than the longitudinal velocity, due to the weak transverse tube coupling. From $\beta = 35$ μJ/g · K^4, and using the microscopic density ρ of 1.3–1.4 g/cm^3, the Debye formula yields $v_{\mathrm{D}} = 1370$ m/s and $v_{\mathrm{T}} \approx 1200$ m/s. On can also directly deduce the value of shear modulus G, from $v_{\mathrm{T}} = (G/\rho)^{1/2}$, which gives $G = 2$ GPa. This is a very small value in comparison to theoretical predictions for *isolated* SWNTs, for instance with $v_{\mathrm{T}} = 9.4$ km/s, and $v_{\mathrm{L}} = 20$ km/s for a (10, 10) NT [15] which yield, with the same microscopic density, a Young modulus Y of 540 GPa and a shear modulus of 120 GPa. In fact, various measurements of individual SWNTs have reported Y values up to 1.2 TPa, but with a broad distribution of data. However, similarly small shear modulus values, between 1 and 3 GPa, were actually measured by direct atomic force microscopy on bundles prepared by AD,

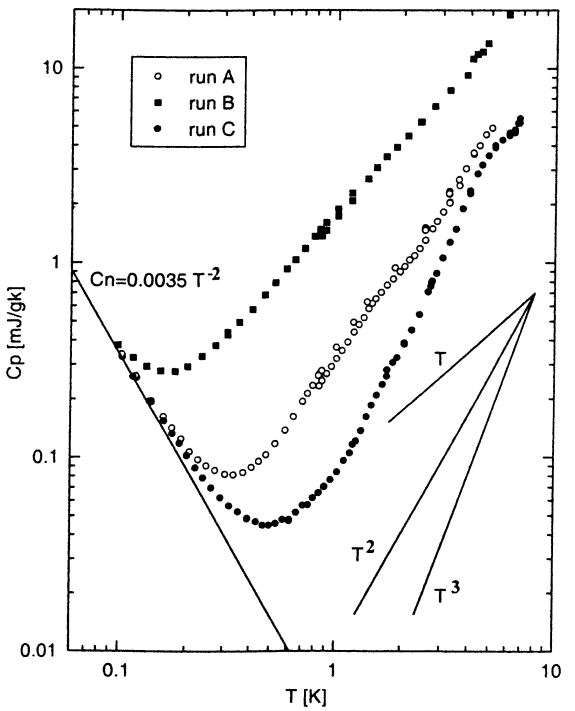

Fig. 7. Log–log plot of the specific heat of the SWNT (laser vaporization) sample for different runs. The role of He^4 adsorption is maximal in run B and minimal in run C. All three runs yield the same nuclear hyperfine contribution C_N (from [13], originally published by American Physical Society).

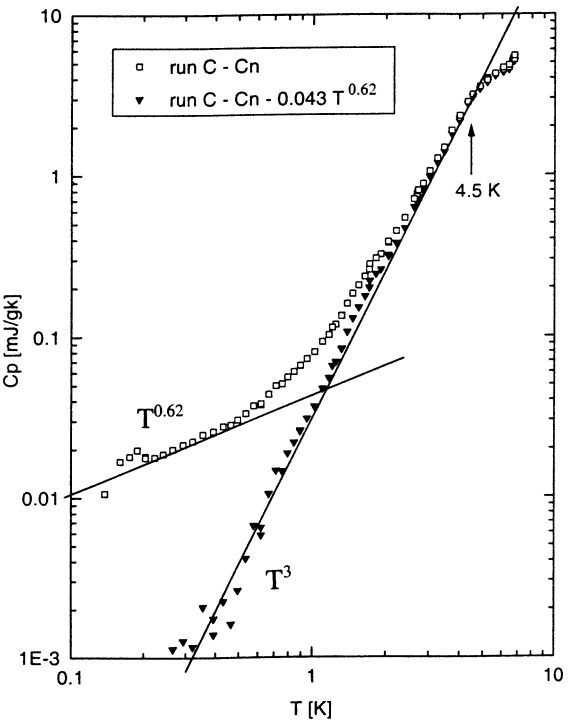

Fig. 8. After subtraction of the nuclear term in run C, the data can be fit with $AT^{0.62} + 0.035T^3$ (mJ/g · K). The vibrational T^3 term is well defined from 0.3 to 4.5 K (from [13], originally published by American Physical Society).

of different diameters between 5 and 20 nm [16]. Such unexpectedly low values were received as bad news for potential applications such as composite materials; they were mostly ascribed to structural imperfections which increase with rope diameter, in particular to the absence of registry between adjacent tubes. Note that the values of Y were rapidly decreasing with rope diameter: from more than 1 TPa for a diameter of less than 3 nm, to around 100–200 GPa above 10 nm.

Coming back to our comparative C_p study, we have obtained similar qualitative behaviour for the AD sample [17]. In that case, due to the absence of the Co catalyst – only Ni and Y – the hyperfine nuclear term was considerably reduced in comparison to the LV sample (see Fig. 10). Again the vibrational contribution can be analysed as the sum of a sub-linear power law corresponding to the localized excitations, plus a T^3 phononic term, both being of larger amplitude than in LV sample (see Fig. 9). We can interpret the larger βT^3, as well as a lower T_{CO} value of $\sim$2 K, in a coherent way, assuming that the transversal lattice cohesion is weaker in bundles of smaller size. This can explain a lower v_T (and a correspoding shear modulus of only 1.1–1.2 GPa included in the low error bar of the AFM measurements [16]) simultaneously to a lower T_{CO}, due to the weaker inter-tube elastic coupling.

Finally, we can make a comment about the experimental values of elastic constants of NTs in different arrangements. Again, the elastic constants (essentially Young modulus or bending modulus, since shear modulus data are very scarce) are extremely sensitive to the diameter of MWNT, or SWNT ropes. Whereas Y is expected to reach 1.2 TPa for *isolated* SWNT, and such high values have indeed been measured in the diameter range 1.0–1.5 nm, with a considerable spread of data from 0.2 to 2.5 GPa [18], it decreases rapidly on increasing diameter in ropes, reaching less than 0.1 TPa for 20 nm diameter [16]. An almost similar trend is observed for the bending modulus of MWNTs: it is as high as 1.2 TPa (as strong as in diamond) for NTs of diameter smaller than 8 nm, but drops to as low as 0.2 TPA for 30 nm, which is ascribed to the wrinkling effect of the wall of the NTs during small bending, an effect which disappears below 12 nm [19]. The mechanical properties are also very sensitive to the method of preparation: at variance with the arc discharge, pyrolisis or vapor deposition techniques seem to cause a high density of defects. In the case of nanotubes fibres, which can reach diameters as large as several tens of μm, Y varies between 9 and 15 Gpa, much larger than for 'bucky paper' mat. [20]. In conclusion, for macroscopic samples, the exceptional mechanical properties of individual or very small ropes of SWNT are rapidly depressed on macroscopic scales.

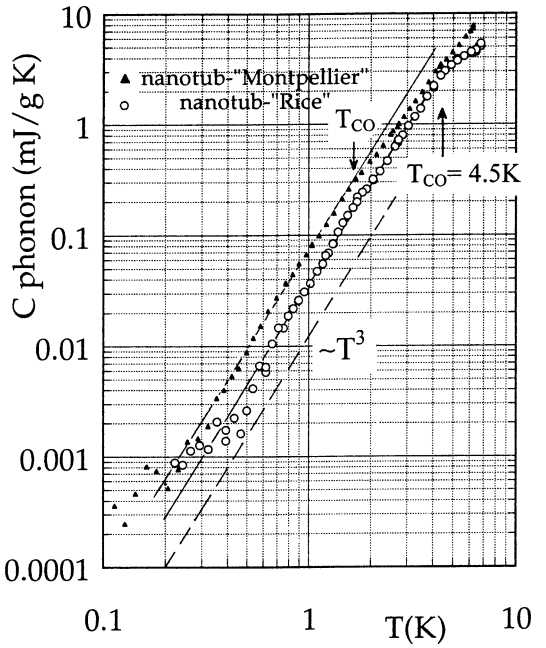

Fig. 9. Comparison of the phonon contribution to C_p in the two kinds of SWNT ropes, prepared either by arc discharge (Montpellier) or laser vaporization (Rice). T_{CO} indicates the phonon dimensionality crossover, from a cubic 3D regime below T_{CO}, and a lower one (2 or 1D) above.

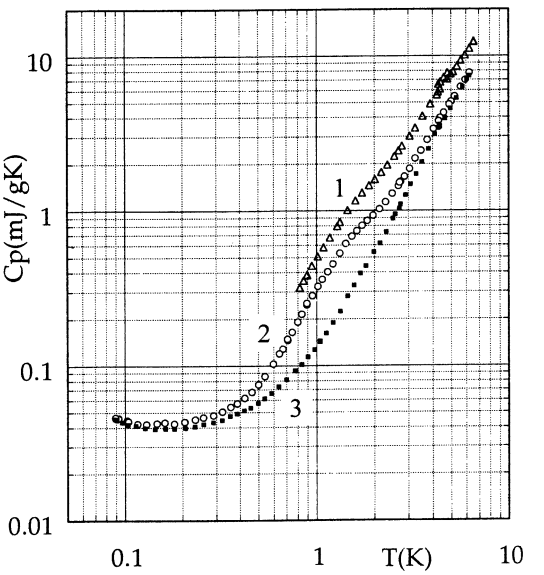

Fig. 10. Specific heat of the arc discharge sample, in successive He^4 desorption states: 1, 2, 3. The state 3 corresponds to the pristine sample (fully outgassed). The upwards low-T deviation below 0.2 K is due to the nuclear hyperfine magnetic contribution (compare to Fig. 7).

4. Heat capacity and adsorption of gases (He^4)

In the field of gas adsorption, hydrogen storage is very important for applications; and there is an article devoted to that question in this present issue. Perhaps of a less useful application, but of considerable academic interest, is He adsorption, interest in which was completely renewed with the advent of NTs. Indeed, we reach here a rich chapter of physics with the properties of quantum fluids He^3 and He^4, in particular their adsorption properties on well defined planar substrates such as graphite. There was a large amount of work already done on this subject, from the 1960s–1970s, which revealed the remarkable properties of both fluids in different phases. We can refer to some basic articles, like the work of Godfrin et al. on He^3 fims on planar graphite in the mK range [21], and the thermodynamics of He^4 adsorbed on graphite or other planar substrates by Greywall et al. [22], Bretz, et al. [23], Elgin and Goodstein [24] etc. The subject was strongly stimulated with carbon NTs, due firstly to the high adsorption ability of their specific surface (~300 m^2/g for individual NTs, ~80 m^2/g for typical bundles of 37 tubes), and secondly to the possibility of 1D confinement in the linear channels of a bundle, a new physics area in comparison to graphite. The problem is rather difficult due to the different available sites to capture He: the external graphene surfaces, the 1D channels like the internal interstitials and the external grooves between two adjacent tubes, characterized by different binding energies [25]. We rule out the case of internal tube adsorption, since they are naturally close-ended, with no possibility for He to enter inside through the surface.

During these last years, there have been many theoretical predictions (see, e.g., the review paper by Calbi et al. [26]), in particular for the properties of He^4 in 1D confinement, a new exciting problem in comparison to grafoil. At variance with the numerous, often contradictory, theoretical papers, there are few experimental data, especially thermodynamics investigations; there are essentially two procedures: the adsorption isotherms on different gases, H_2, D_2, CH_4, He, and the desorption experiments, not strictly calorimetric in nature. Measurements of adsorption isotherms enable one to determine, from the successive steps in the isotherms, the distinct sites of adsorption, with different heats of adsorption; in the case of He^4 [27] the 1D channels (outer grooves) were detected as having the highest binding energy, then the outer surfaces with successive layers coverage, as in graphite. Desorption experiments [28,29] are more difficult to interpret, but the conclusions are that the interstitial channels are the most attractive sites.

We have measured the heat capacity of the two kinds of SWNT bundles with adsorbed He^4. The first example (LV sample) was shown in a previous paragraph (Fig. 7); we have also investigated the AD sample with similar levels of adsorbate [30]. Fig. 10 shows the progressive evolution of the total specific heat (per g of sample) under successive steps of desorption, with

contents of He rather similar – within a factor of 2 – to the previous case of the LV sample; present states 1, 2, 3 correspond to states B, A, C for LV sample, with run 3 for the totally outgassed state. We immediately see that the anomaly of He in run 2 is well developed in our T-range investigated. One can define the specific heat of the adsorbate by subtracting for each run the reference state, which is that of pristine NT: this is possible due to the very weak interaction of He atoms with the carbon lattice. The result is that both samples show an overall similar qualitative behaviour, but with differences at very low temperature (<1 K), that we can interpret [30] by differences in the ropes morphology, i.e., difference in size, and hence in the ratio 1D sites/surfaces sites. For instance, we have detected in the AD sample a low-T regime which decreases exponentially, like an Einstein specific heat. This is strongly indicative of the 1D He confinement, the localized He atoms being treated as harmonic oscillators, contrary to a 2D fluid regime which is expected to occur for adsorption on external surfaces; for the latter case, one expects a T^2 Debye regime.

Finally, we reached a coherent interpretation of both the vibrational (propagative phonons) and the He adsorbate contributions, by taking into account the different morphology – essentially the mean number of tubes per bundle – of the two different kinds of samples.

Acknowledgements

Thermal experiments and their analysis were realised in collaboration with K. Biljakovic (Institute of Physics, Zagreb), and with the help of P. Monceau (CRTBT). I am grateful for many instructive and fruitful discussions with the Montpellier group, J.L. Sauvajol, R. Almairac, S. Rols, and N. Bendiab, who also performed the characterization experiments. I also thank J.E. Fischer (Pennsylvania University) for his collaboration during the first part of this study.

References

[1] J. Hone, M. Whitney, C. Piskotti, A. Zettl, Phys. Rev. B 59 (1999) R2514.
[2] S. Berber, Y.K. Kwon, D. Tomanek, Phys. Rev. Lett. 84 (2000) 4613.
[3] W. Yi, L. Lu, Z. Dian-Lin, Z.W. Pan, S.S. Xie, Phys. Rev. B 59 (1999) R9015.
[4] J.E. Fischer, W. Zhou, J. Vavro, M.C. Llaguno, C. Guthy, R. Haggenmueller, M.J. Casavant, D.E. Walters, R.E. Smalley, J. Appl. Phys. 93 (2003) 2157.
[5] P. Kim, Li Shi, A. Majumdar, P.L. McEuen, Phys. Rev. Lett. 87 (2001) 215502;
P. Kim, Li Shi, A. Majumdar, P.L. McEuen, Physica B 323 (2002) 67.
[6] K. Schwab, E.A. Henriksen, J.M. Worlock, M.L. Roukes, Nature 404 (2000) 974.
[7] J. Hone, B. Batlogg, Z. Benes, A.T. Johnson, J.E. Fischer, Science 289 (2000) 1730.
[8] S.M. Genensky, G.F. Newell, J. Chem. Phys. 26 (1957) 486.
[9] S. Rols, Z. Benes, E. Anglaret, J.L. Sauvajol, P. Papanek, J.E. Fischer, G. Coddens, H. Schober, A.J. Dianoux, Phys. Rev. Lett. 85 (2000) 5222.
[10] S. Rols, Thesis, Université de Montpellier (2000);
J.L. Sauvajol, E. Anglaret, S. Rols, L. Alvarez, Carbon 40 (2002) 1697.
[11] A. Thess, et al., Science 273 (1996) 483.
[12] C. Journet, et al., Nature 388 (1997) 756.
[13] J.C. Lasjaunias, K. Biljakovic, Z. Benes, J.E. Fischer, P. Monceau, Phys. Rev. B 65 (2002) 113409.
[14] A. Mizel, L.X. Benedict, M.L. Cohen, S.G. Louie, A. Zettl, N.K. Budraa, W.P. Byermann, Phys. Rev. B 60 (1999) 3264.
[15] R. Saito, T. Takeya, T. Kimura, G. Dresselhaus, M.S. Dresselhaus, Phys. Rev. B 57 (1998) 4145.
[16] J.P. Salvetat, G.A.D. Briggs, J.M. Bonard, R.R. Bacsa, A.J. Kulik, T. Stockli, N.A. Burnham, L. Forro, Phys. Rev. Lett. 82 (1999) 944.
[17] J.C. Lasjaunias, K. Bijakovic, P. Monceau, J.L. Sauvajol, et al., Nanotechnology 14 (2003), in press.
[18] A. Krishnan, E. Dujardin, T.W. Ebbesen, P.N. Yianilos, M.M.J. Treacy, Phys. Rev. B 58 (1998) 14013.
[19] Z.L. Wang, R.P. Gao, P. Poncharal, W.A. de Heer, Z.R. Dai, Z.W. Pan, Mat. Sci. Engin. C 16 (2001) 3.
[20] B. Vigolo, et al., Mat. Res. Soc. Symp. Proc. 633 (2001) A12-1.
[21] H. Godfrin, H.J. Lauter, Experimental properties of He^3 adsorbed on graphite, in: W.P. Halperin (Ed.), in: Progress in Low-Temperature Physics, Vol. 14, Elsevier, 1995.
[22] D.S. Greywall, P.A. Busch, Phys. Rev. Lett. 67 (1991) 3535;
D.S. Greywall, Phys. Rev. B 47 (1993) 309.
[23] M. Bretz, J.G. Dash, D.C. Hickernell, E.O. McLean, O.E. Vilches, Phys. Rev. A 8 (1973) 1589.
[24] R.L. Elgin, D.L. Goodstein, Phys. Rev. A 9 (1974) 2657.
[25] G. Stan, M.J. Bojan, S. Curtarolo, S.M. Gatica, M.W. Cole, Phys. Rev. B 62 (2000) 2173.
[26] M. Calbi, M.W. Cole, S.M. Gatica, M.J. Bojan, G. Stan, Rev. Modern Phys. 73 (2001) 857.
[27] T. Wilson, O.E. Vilches, Low Temperature Physics-23, Proc. of LT 23 Conf., August 2002, Physica B 329–333 (2003) 278.
[28] W. Teizer, R.B. Hallock, E. Dujardin, T.W. Ebbessen, Phys. Rev. Lett. 82 (1999) 5305;
Erratum, W. Teizer, R.B. Hallock, E. Dujardin, T.W. Ebbessen, Phys. Rev. Lett. 84 (2000) 1844.
[29] Y.H. Kahng, R.B. Hallock, E. Dujardin, T.W. Ebbessen, J. Low Temp. Phys. 126 (2002) 223.
[30] J.C. Lasjaunias, K. Biljakovic, J.L. Sauvajol, P. Monceau, Phys. Rev. Lett. 91 (2003) 025901.